

New Journal of Chemistry

Supplementary Material

Structural, spectroscopic and theoretical studies on dixanthogens: (ROC(S)S)₂, with R = n-propyl and isopropyl

*Luciana C. Juncal, Yeny A. Tobón, Oscar E. Piro, Carlos O. Della Védova and
Rosana M. Romano**

Table S1. Crystal data and structure refinement results for [(CH₃)₂CHOC(S)S]₂.

Empirical formula	C ₈ H ₁₄ O ₂ S ₄
Formula weight	270.43
Temperature	296(2) K
Wavelength	1.54184 Å
Crystal system	Monoclinic
Space group	<i>P</i> 2 ₁ / <i>c</i>
Unit cell dimensions	<i>a</i> = 9.735(1) Å <i>b</i> = 12.588(3) Å <i>c</i> = 12.131(2) Å β = 112.65(1)°
Volume	1371.9(4) Å ³
Z, calculated density	4, 1.309 Mg/m ³
Absorption coefficient	6.186 mm ⁻¹
F(000)	568
Crystal size	0.36 x 0.24 x 0.20 mm ³
ϑ -range for data collection	4.92 to 68.00°
Index ranges	11 ≤ <i>h</i> ≤ 0, -1 ≤ <i>k</i> ≤ 15, -13 ≤ <i>l</i> ≤ 14
Reflections collected	2798
Independent reflections	2408 [R(int) = 0.0572]
Observed reflections [I > 2σ(I)]	1984
Completeness to ϑ = 68.00°	96.4%
Max. and min. transmission	0.4126 and 0.1587
Refinement method	Full-matrix least-squares on F ²
Data / restraints / parameters	2408 / 0 / 131
Goodness-of-fit on F ²	1.065
Final R indices [I > 2σ(I)]	R1 = 0.0720, wR2 = 0.1911
R indices (all data)	R1 = 0.0806, wR2 = 0.2066
Largest diff. peak and hole	0.769 and -0.474 e.Å ⁻³

$$^a R_1 = \frac{\sum ||F_o| - |F_c||}{\sum |F_o|}, \quad wR_2 = \left[\frac{\sum w(|F_o|^2 - |F_c|^2)^2}{\sum w(|F_o|^2)^2} \right]^{1/2}$$

Table S2 Atomic coordinates ($\times 10^4$) and equivalent isotropic displacement parameters ($\text{\AA}^2 \times 10^3$) for $[(\text{CH}_3)_2\text{CHOC}(\text{S})\text{S}]_2$. $U(\text{eq})$ is defined as one third of the trace of the orthogonalized U_{ij} tensor.

Atom	x	y	z	$U(\text{eq})$
S(1)	8205(1)	885(1)	-78(1)	81(1)
S(2)	6946(1)	-450(1)	-686(1)	78(1)
S(3)	9701(2)	2389(1)	-1001(1)	117(1)
S(4)	3849(1)	-941(1)	-1949(1)	91(1)
O(1)	8069(4)	795(2)	-2244(2)	86(1)
O(2)	4956(3)	1016(2)	-1523(2)	68(1)
C(1)	8657(4)	1342(3)	-1266(3)	73(1)
C(2)	5099(4)	-4(3)	-1444(3)	69(1)
C(3)	8360(6)	1075(4)	-3326(4)	91(1)
C(4)	3463(4)	1482(3)	-2153(3)	72(1)
C(5)	6890(7)	1147(6)	-4317(5)	139(3)
C(6)	3180(6)	1528(4)	-3462(4)	98(1)
C(7)	9323(7)	217(7)	-3491(6)	139(2)
C(8)	3505(6)	2544(3)	-1607(4)	91(1)

Table S3. Full bond lengths [\AA] and angles [$^\circ$] for $[(\text{CH}_3)_2\text{CHOC}(\text{S})\text{S}]_2$

S(1)-C(1)	1.758(4)	C(2)-S(2)-S(1)	106.0(1)
S(1)-S(2)	2.042(2)	C(1)-O(1)-C(3)	120.9(3)
S(2)-C(2)	1.767(4)	C(2)-O(2)-C(4)	119.3(3)
S(3)-C(1)	1.619(4)	O(1)-C(1)-S(3)	129.4(3)
S(4)-C(2)	1.635(4)	O(1)-C(1)-S(1)	114.5(3)
O(1)-C(1)	1.298(4)	S(3)-C(1)-S(1)	116.1(2)
O(1)-C(3)	1.488(5)	O(2)-C(2)-S(4)	130.3(3)
O(2)-C(2)	1.291(4)	O(2)-C(2)-S(2)	114.4(3)
O(2)-C(4)	1.478(4)	S(4)-C(2)-S(2)	115.3(2)
C(3)-C(5)	1.475(8)	C(5)-C(3)-O(1)	106.3(4)
C(3)-C(7)	1.493(8)	C(5)-C(3)-C(7)	113.4(5)
C(4)-C(6)	1.504(5)	O(1)-C(3)-C(7)	106.9(4)
C(4)-C(8)	1.487(6)	O(2)-C(4)-C(6)	107.8(3)
		O(2)-C(4)-C(8)	105.9(3)
C(1)-S(1)-S(2)	106.1(1)	C(6)-C(4)-C(8)	113.5(4)

Table S4. Anisotropic displacement parameters ($\text{\AA}^2 \times 10^3$) for $[(\text{CH}_3)_2\text{CHOC}(\text{S})\text{S}]_2$. The anisotropic displacement factor exponent takes the form: $-2\pi^2[h^2a^{*2}U^{11} + \dots + 2hk a^*b^*U^{12}]$.

Atom	U^{11}	U^{22}	U^{33}	U^{23}	U^{13}	U^{12}
S(1)	76(1)	104(1)	55(1)	-6(1)	17(1)	4(1)
S(2)	91(1)	78(1)	70(1)	12(1)	36(1)	13(1)
S(3)	111(1)	125(1)	110(1)	-34(1)	37(1)	-50(1)
S(4)	102(1)	76(1)	106(1)	-10(1)	54(1)	-16(1)
O(1)	109(2)	88(2)	65(2)	-14(1)	39(2)	-28(2)
O(2)	72(1)	69(1)	60(1)	6(1)	20(1)	-2(1)
C(1)	61(2)	85(2)	66(2)	-6(2)	17(2)	2(2)
C(2)	80(2)	77(2)	58(2)	2(2)	36(2)	0(2)
C(3)	120(4)	92(3)	71(2)	-6(2)	47(2)	-27(3)
C(4)	67(2)	77(2)	69(2)	9(2)	24(2)	0(2)
C(5)	143(5)	199(7)	79(3)	25(4)	47(3)	61(5)
C(6)	109(3)	105(3)	63(2)	7(2)	15(2)	7(3)
C(7)	104(4)	210(7)	124(5)	22(5)	68(4)	32(5)
C(8)	102(3)	83(3)	97(3)	3(2)	48(3)	7(2)

Table S5. Hydrogen coordinates ($\times 10^4$) and isotropic displacement parameters ($\text{\AA}^2 \times 10^3$) for $[(\text{CH}_3)_2\text{CHOC}(\text{S})\text{S}]_2$

Atom	x	y	z	U(eq)
H(3)	8874	1760	-3211	109
H(4)	2709	1037	-2030	86
H(5A)	6410	467	-4441	209
H(5B)	7016	1362	-5032	209
H(5C)	6289	1661	-4124	209
H(6A)	3925	1962	-3576	147
H(6B)	2214	1829	-3893	147
H(6C)	3220	824	-3751	147
H(7A)	8809	-450	-3609	208
H(7B)	10230	176	-2795	208
H(7C)	9550	375	-4177	208
H(8A)	3812	2469	-758	137
H(8B)	2532	2858	-1933	137
H(8C)	4198	2992	-1776	137

Table S6. Torsion angles [°] for [(CH₃)₂CHOC(S)S]₂

C(1)-S(1)-S(2)-C(2)	-85.0(2)
C(3)-O(1)-C(1)-S(3)	2.3(6)
C(3)-O(1)-C(1)-S(1)	-179.3(3)
S(2)-S(1)-C(1)-O(1)	3.0(3)
S(2)-S(1)-C(1)-S(3)	-178.4(2)
C(4)-O(2)-C(2)-S(4)	0.1(5)
C(4)-O(2)-C(2)-S(2)	179.2(2)
S(1)-S(2)-C(2)-O(2)	4.4(3)
S(1)-S(2)-C(2)-S(4)	-176.4(2)
C(1)-O(1)-C(3)-C(5)	-128.8(5)
C(1)-O(1)-C(3)-C(7)	109.8(5)
C(2)-O(2)-C(4)-C(6)	-85.7(4)
C(2)-O(2)-C(4)-C(8)	152.5(3)

Table S7. Comparison of the ^1H NMR chemical shifts (δ , in ppm) of different dixanthogen molecules

Compound	δ CH ₃ .	δ CH ₂	δ CH ₂ -O	Reference
[CH ₃ CH ₂ OC(S)S] ₂	1.42 (t, J=7.2)	-	4.70 (q, J=7.2)	Reference 2
[CH ₃ (CH ₂) ₂ OC(S)S] ₂	0.98 (t, J=7.3)	1.73-1.91 (m)	4.55 (t, J=6.3)	This work
[(CH ₃) ₂ CHOC(S)S] ₂	1.40 (d, J= 3.2)	-	-	Reference 2
[(CH ₃) ₂ CHCH ₂ OC(S)S] ₂	1.0 (d, J= 6.8)	-	4.36 (d, J=7.2)	Reference 2

Table S8. Comparison of the ^{13}C NMR chemical shifts (δ , in ppm) of different dixanthogen molecules

Compound	δ CH ₃ .	δ CH ₂	δ CH ₂ -O	δ CS ₂	Reference
[CH ₃ CH ₂ OC(S)S] ₂	13.8	-	71.8	207.1	Reference 2
[CH ₃ (CH ₂) ₂ OC(S)S] ₂	10.7	21.8	76.7	207.6	This work
[(CH ₃) ₂ CHOC(S)S] ₂	21.3	-	-	207.1	Reference 2
[(CH ₃) ₂ CHCH ₂ OC(S)S] ₂	19.1	-	81.3	207.1	Reference 2

Table S9. Parameters used in the gas Chromatography – Mass Spectrometry measurements

Carrier gas:	He	
Column:	19091J-433 HP-5	
Length:	30 m	
I.D:	0.25 mm	
Film:	0.25 μm	
Injection volume:	1 μl	
Column oven temperature:	100 $^{\circ}\text{C}$	
Injection temperature:	200 $^{\circ}\text{C}$	
Injection mode:	Split	
Flow control mode:	Pressure	
Pressure:	120.0 kPa	
Total flow:	43.8 ml/min	
Column flow:	1.94 ml/min	
Linear velocity:	50.9 cm/s	
Purge flow:	3.0 ml/min	
Split ratio:	20.0	
Oven temperature program:		
Rate ($^{\circ}\text{C}/\text{min}$)	Temperature ($^{\circ}\text{C}$)	Hold time (min)
-	100	2
20	150	1
25	300	2
Ions source temperature:	200.0 $^{\circ}\text{C}$	
Interface temperature:	250.0 $^{\circ}\text{C}$	
Solvent cut time:	3 min	
Acquisition mass range:	2 - 500	
Ionization energy:	70 eV	

Table S10. Fragments observed in the mass spectra of $[\text{CH}_3(\text{CH}_2)_2\text{OC}(\text{S})\text{S}]_2$ and $[(\text{CH}_3)_2\text{CHOC}(\text{S})\text{S}]_2$, relative intensity and assignment

m/z	Relative Intensity		Assignment
	$[\text{CH}_3(\text{CH}_2)_2\text{OC}(\text{S})\text{S}]_2$	$[(\text{CH}_3)_2\text{CHOC}(\text{S})\text{S}]_2$	
15	0.7	0.9	CH_3^+
26	0.8	-	C_2H_2^+
27	19.0	10.1	C_2H_3^+
28	2.5	1.4	$\text{C}_2\text{H}_4^+ / \text{CO}^+$
29	2.5	-	CH_3CH_2^+
30	0.3	-	CH_2O^+
31	1.3		CH_3O^+
32	1.9	1.6	S^+
38	-	0.5	C_3H_2^+
39	6.2	3.6	C_3H_3^+
40	0.9	0.8	C_3H_4^+
41	33.2	19.5	C_3H_5^+
42	3.4	3.0	$\text{C}_3\text{H}_6^+ / \text{C}_2\text{H}_2\text{O}^+$
43	100.0	100.0	C_3H_7^+
44	4.1	4.1	CS^+
45	1.1	1.6	CHS^+
47	0.9	-	CH_3S^+
59	0.5	1.2	$\text{C}_3\text{H}_7\text{O}^+$
60	1.9	3.8	OCS^+
61	0.8	0.8	OCSH^+
64	1.5	1.0	SS^+
65	0.5	-	S_2H^+
66	2.4	2.7	S_2H_2^+
75	1.4	1.2	$\text{C}_3\text{H}_7\text{S}^+$
76	5.1	3.8	CS_2^+
77	1.4	0.6	CS_2H^+
78	0.7	-	CS_2H_2^+
92	0.7	-	OCS_2^+

m/z	Relative Intensity		Assignment
	$[\text{CH}_3(\text{CH}_2)_2\text{OC}(\text{S})\text{S}]_2$	$[(\text{CH}_3)_2\text{CHOC}(\text{S})\text{S}]_2$	
93	0.8	1.1	OCS_2H^+
95	0.7	-	CH_3OSS^+
103	2.7	3.0	$\text{C}_3\text{H}_7\text{OCS}^+$
108	8.0	16.4	CS_3^+
109	0.5	0.8	CS_3H^+
110	0.8	1.5	CS_3H_2^+
126	-	1.2	OCS_3H_2^+
135	0.5	-	$\text{C}_3\text{H}_7\text{OCS}_2^+$
136	0.6	0.8	OC_2S_3^+
168	2.8	5.4	OC_2S_4^+
270	0.8	0.8	$\text{M}^+, [\text{C}_3\text{H}_7\text{OCS}_2]^+$

Table S11. Dihedral angles and relative energies of the most stable conformations of [CH₃(CH₂)₂OC(S)S]₂ calculated with the B3LYP/6-31+G* approximation

Conformer	$\tau_{C(9)C(6)C(3)O(2)}$	$\tau_{C(6)C(3)O(2)C(1)}$	$\tau_{S(14)C(1)S(13)S(18)}$	$\tau_{C(1)S(13)S(18)C(16)}$	$\tau_{S(13)S(18)C(16)S(15)}$	$\tau_{C(16)O(17)C(19)C(22)}$	$\tau_{O(17)C(19)C(22)C(25)}$	ΔE (kcal mol ⁻¹)
I (AAAGAAA)	179.9	-178.9	177.1	85.1	177.1	-178.9	179.9	0.00
II (AAAGAAG ⁺)	179.9	-178.5	177.1	84.2	177.0	-178.6	65.0	0.08
III (G ⁺ AAGAAG ⁻)	64.6	-178.5	177.4	86.6	177.6	-178.1	-65.4	0.26
IV (AASGAAA)	179.9	179.8	-6.3	85.3	176.3	179.0	180.0	1.54
V (AAAGSAG ⁺)	179.6	-179.1	176.5	85.6	-5.5	-179.0	65.4	1.58
VI (AASGAAG ⁺)	-179.9	-179.0	-5.0	85.3	176.4	-179.8	64.5	1.59
VII (G ⁺ AAGSAG ⁻)	64.4	-179.7	176.6	85.5	-5.2	-179.1	-64.4	1.66
VIII (G ⁺ ASGAAG ⁻)	65.5	180.0	-6.3	87.4	175.1	178.1	-67.0	1.80
IX (AASGSAA)	180.0	-179.6	-3.3	88.8	-3.3	-179.5	180.0	2.84
X (AASGSAG ⁺)	179.9	-179.6	-2.5	88.9	-3.7	-179.7	64.7	2.92
XI (G ⁺ ASGSAG ⁻)	65.0	-179.1	-2.9	88.7	-2.6	-179.3	-64.7	2.98

A, S and G denote *anti*, *syn* and *gauche*, respectively

Table S12. Dihedral angles and relative energies of the most stable conformations of $[(\text{CH}_3)_2\text{CHOC}(\text{S})\text{S}]_2$ calculated with the B3LYP/6-31+G* approximation

Conformer	$\tau_{\text{S}(13)\text{C}(12)\text{S}(14)\text{S}(15)}$	$\tau_{\text{C}(12)\text{S}(14)\text{S}(15)\text{C}(16)}$	$\tau_{\text{S}(14)\text{S}(15)\text{C}(16)\text{S}(17)}$	ΔE (kcal mol ⁻¹)
I (AGA)	178.1	86.2	178.1	0.00
II (SGA)	-6.9	86.7	175.5	1.56
III (SGS)	-2.7	89.2	-2.8	2.90

A, S and G denote *anti*, *syn* and *gauche*, respectively

Table S13. Net atomic charges obtained by Mulliken population analysis and dipole moments and of $[\text{CH}_3(\text{CH}_2)_2\text{OC}(\text{S})\text{S}]_2$ and $[(\text{CH}_3)_2\text{CHOC}(\text{S})\text{S}]_2$, calculated with the B3LYP/6-31+G* approximation

Atom	Net Charge [e]	
	$[\text{CH}_3(\text{CH}_2)_2\text{OC}(\text{S})\text{S}]_2$	$[(\text{CH}_3)_2\text{CHOC}(\text{S})\text{S}]_2$
S(1)	0.273	0.279
S(2)	0.273	0.279
C(1)	-0.318	-0.272
C(2)	-0.318	-0.272
S(3)	-0.044	-0.169
S(4)	-0.044	-0.169
O(1)	0.139	-0.071
O(2)	0.139	-0.071
C(3)	-0.127	-0.127
H(3A)	0.228	0.241
H(3B)	0.224	-
C(4)	-0.127	-0.127
H(4A)	0.228	0.241
H(4B)	0.224	-
C(5)	-0.506	-0.585
H(5A)	0.206	0.228
H(5B)	0.217	0.230
H(5C)	-	0.231
C(6)	-0.506	-0.585
H(6A)	0.206	0.228
H(6B)	0.217	0.230
H(6C)	-	0.231
C(7)	-0.651	-0.669
H(7A)	0.203	0.221
H(7B)	0.231	0.229
H(7C)	0.205	0.233
C(8)	-0.651	-0.669

continuation of the Table S13

Atom	Net Charge [e]	
	$[\text{CH}_3(\text{CH}_2)_2\text{OC}(\text{S})\text{S}]_2$	$[(\text{CH}_3)_2\text{CHOC}(\text{S})\text{S}]_2$
H(8A)	0.203	0.221
H(8B)	0.231	0.229
H(8C)	0.205	0.233
Dipole moment (μ , Debye)	3.66	4.69

Table S14. Experimental (IR and Raman) and calculated (for the most stable conformers) wavenumbers (cm⁻¹), relative intensities and tentative assignments of [CH₃(CH₂)₂OC(S)S]₂

Experimental		B3LYP/6-31+G*									Assignment
		Structure I			Structure II			Structure III			
IR	Ra	ν	I _{IR}	I _{Raman}	ν	I _{IR}	I _{Raman}	ν	I _{IR}	I _{Raman}	
2969	2970	3129	5	9	3129	4	19	3130	5	18	v _{as} CH ₃ ; v _{as} CH ₂
		3129	7	2	3129	7	13	3129	4	26	
					3127	3	18	3128	1	15	
								3128	6	28	
2948	2948	3119	8	34	3119	4	67				
		3119	<1	36							
2936	2934				3110	4	42	3110	5	41	
								3110	4	44	
2922		3107	3	5	3107	4	5				
		3107	4	<1							
2885	2878	3084	<1	49	3084	<1	68	3083	2	80	
		3084	<1	24	3080	3	71	3081	3	69	
2878		3073	2	40	3073	2	38	3071	<1	60	
		3073	3	1	3070	<1	57	3070	<1	57	
2852	2852	3055	3	8	3055	2	55	3047	4	97	v _s CH ₃ ; v _{as} CH ₂ ; v _{as} CH ₂
		3055	1	50	3047	4	100	3046	3	100	
		3044	4	100	3044	4	94	3043	4	88	
		3044	4	<1	3041	3	82	3042	4	80	
2776											
2738	2737										
2682											
2613											
2506											
2288											
2049											
1948											
1916											

Overtone and Combination Bands

continuation of the Table S14

Experimental		B3LYP/6-31+G*									Assignment
		Structure I			Structure II			Structure III			
IR	Ra	ν	I_{IR}	I_{Raman}	ν	I_{IR}	I_{Raman}	ν	I_{IR}	I_{Raman}	
1143		1186	<1	<1	1187	<1	1	1174	1	1	
		1186	<1	1	1173	1	1	1173	1	<1	
1130		1152	4	1	1152	4	2				
		1151	4	1							
1103					1130	3	1	1130	2	1	
								1130	4	1	
1049					1071	8	3	1072	8	3	
								1069	6	2	
1036	1036	1060	24	18	1055	23	30	1047	18	37	
		1051	11	4							
		1049	4	5	1049	6	9				
1018	1018 sh	1042	77	1	1036	75	6	1032	85	3	
934	934										
920	918	954	12	1	953	7	5				
		953	2	5							
894	888				939	3	3	939	5	3	
								937	2	3	
								911	3	4	
								910	1	3	
865	865	902	1	1	909	2	4				
		902	<1	2	903	<1	<1				
		902	<1	9	902	2	13				
		902	3	3							
856					873	1	10	874	2	2	
								874	<1	19	
770	767				780	1	<1	781	1	<1	
								778	1	<1	
758		768	<1	<1	770	<1	<1				
		768	<1	<1							
690	688	699	1	<1	699	1	2				

continuation of the Table S14

Experimental		B3LYP/6-31+G*									Assignment
		Structure I			Structure II			Structure III			
IR	Ra	ν	I _{IR}	I _{Raman}	ν	I _{IR}	I _{Raman}	ν	I _{IR}	I _{Raman}	
		699	<1	3							
	670				695	<1	4	695	<1	3	
								694	<1	4	
648	648	570	<1	<1	570	<1	<1	571	<1	1	δ OCS _{i.p.}
617		546	<1	<1	546	<1	<1	547	<1	<1	δ OCS _{o.f.p.}
564	561	496	<1	2	492	<1	4				δ OCS _{i.p.}
542	543	487	<1	1							δ OCS _{o.f.p.}
530	529				461	<1	17	471	<1	20	ν S-S
								450	<1	<1	δ OCS
	498	444	<1	25							ν S-S
					442	<1	18	442	<1	14	ρ CH ₃
	478							426	1	4	δ OCS
454	451				419	<1	18	413	<1	24	
423	423	359	1	1	356	1	5				δ COC
		353	1	4							
414								328	1	<1	
394		320	1	1	325	1	2				δ SCS; δ CCC
360	360				302	<1	5	309	<1	4	
326	325	291	<1	6				291	<1	4	τ HCCC
	307	270	1	<1	277	1	4				δ SCS; δ CCC
291		235	<1	<1	239	<1	<1	235	<1	8	
		235	<1	<1							τ HCCC
274					226	<1	5	221	1	1	
240		208	<1	3	215	<1	1	215	<1	1	δ SCS
220	221	192	<1	1	194	<1	3	193	<1	<1	τ COCS

Table S15. Experimental (IR and Raman) and calculated (for the most stable conformer) wavenumbers (cm^{-1}), relative intensities and tentative assignments of $[(\text{CH}_3)_2\text{CHOC}(\text{S})\text{S}]_2$

Experimental		B3LYP/6-31+G*			Assignment
FTIR	FT-Raman	ν	I_{IR}	I_{Raman}	
		3141	4	7	
		3141	<1	5	
2979	2982	3135	5	18	
		3135	2	1	
2952		3129	2	7	$\nu_{\text{as}} \text{CH}_3$
	2949	3129	8	39	
2932	2935	3121	<1	4	
		3121	<1	1	
		3101	<1	4	$\nu \text{C-H}_{\text{o.f.p.}}$
2920	2920	3101	<1	11	$\nu \text{C-H}_{\text{i.p.}}$
		3059	2	100	
2895	2895	3059	4	4	
	2869	3055	1	2	$\nu_{\text{s}} \text{CH}_3$
2871		3055	3	<1	
2816					
2742	2743				
2732	2733				
2602					$\nu \text{O-C}_{\text{o.f.p.}} + \delta \text{H-C-O}_{\text{i.p.}}$
2532					$2 \nu \text{O-C}_{\text{o.f.p.}}$
2353					$\nu \text{O-C}_{\text{o.f.p.}} + \delta \text{CH}_3\text{-C}$
2270					$\nu \text{O-C}_{\text{o.f.p.}} + \nu \text{C=S}_{\text{o.f.p.}}$
2078					
2022					$\nu \text{C=S}_{\text{o.f.p.}} + \nu \text{C=S}_{\text{i.p.}}$
1956					$\nu \text{O-C}_{\text{o.f.p.}} + \nu \text{C-S}_{\text{o.f.p.}}$
1878					
1837					
1798					
1774					
1703					
1689					$\nu \text{C=S}_{\text{o.f.p.}} + \nu \text{C-S}_{\text{o.f.p.}}$
1589					$2 \nu \text{C-O}_{\text{o.f.p.}}$
		1531	1	<1	
1465		1530	2	<1	
		1518	<1	5	
1457	1453	1518	2	1	
		1508	<1	4	$\delta \text{H-C-H}$
1448	1445	1508	<1	1	
		1504	<1	<1	
1419		1503	<1)	<1	
		1444	<1	<1	
1387	1387	1444	4	<1	δCH_3
		1429	1	<1	
1373		1428	5	<1	

Experimental		B3LYP/6-31+G*			Assignment
FTIR	FT-Raman	ν	I_{IR}	I_{Raman}	
1354	1351	1393	3	2	δ H-C-O _{i.p.}
		1391	3	1	δ H-C-O _{o.f.p.}
1341	1340	1381	<1	1	δ H-C-C
		1381	2	<1	
	1278	1306	26	2	ν O-C _{i.p.}
1272	1268	1301	100	<1	ν O-C _{o.f.p.}
1186		1213	1	<1	δ CH ₃ -C
	1185	1213	<1	1	
1146	1147	1169	<1	<1	ν_{as} C-C-C _{i.p.}
		1169	4	1	ν_{as} C-C-C _{o.f.p.}
1092	1089	1128	22	1	δ CH ₃ -C
1083		1123	27	<1	
1027	1019	1032	18	11	ν C=S _{i.p.}
1003	1003	1016	94	1	ν C=S _{o.f.p.}
939	942	958	<1	<1	δ CH ₃ -C
		958	1	<1	
934	934	948	<1	<1	
		948	<1	<1	
898	899	912	4	2	ν_s C-C-C _{o.f.p.}
		912	2	<1	ν_s C-C-C _{i.p.}
795		806	4	<1	ν C-O _{o.f.p.}
	796	804	<1	4	ν C-O _{i.p.}
690	691	694	1	<1	ν C-S _{o.f.p.}
		694	<1	2	ν C-S _{i.p.}
567	566	572	<1	<1	δ_{oop} C=S _{o.f.p.}
545	548	549	<1	<1	δ_{oop} C=S _{i.p.}
	501	478	<1	3	ν S-S
468	467	464	<1	<1	δ O-C=S _{o.f.p.}
	457	450	<1	6	δ C-O-C _{i.p.}
		443	1	<1	δ C-O-C _{o.f.p.}
443	444	434	1	6	δ S=C-S _{i.p.}
396		391	1	<1	δ C-C-O _{o.f.p.}
384	382	385	<1	3	δ C-C-O _{i.p.}
331	330	328	<1	<1	δ C-C-C _{o.f.p.}
		326	<1	1	δ C-C-C _{i.p.}
305	302	301	1	<1	δ S=C-S _{o.f.p.}
257	254	252	<1	1	τ H-C-C-H
	248	247	<1	<1	
219	219	212	<1	1	δ O-C=S _{i.p.}
		211	<1	<1	τ H-C-C-H
206		210	<1	<1	
		196	1	<1	τ C-C-O-C
200	200	190	<1	3	
		142	126	<1	1
	128	114	<1	<1	

Table S16. Wavelength (λ , nm) and oscillator strength of the mono-electronic transitions of $[\text{CH}_3(\text{CH}_2)_2\text{OC}(\text{S})\text{S}]_2$ calculated with the TD-B3LYP/6-31+g (d) approximation

N°	$\lambda(\text{nm})$	Oscillator Strength	Major contribution	Minor contribution
5	280.5	0.047	H-2->L+2 (40%), H-1->L+1 (35%), HOMO->LUMO (19%)	
9	265.3	0.1661	H-3->L+1 (38%), H-2->LUMO (12%), H-2->L+2 (20%), HOMO->LUMO (11%), HOMO->L+2 (10%)	H-1->L+1 (3%)
11	249.3	0.7099	H-3->L+1 (48%), H-2->LUMO (10%), HOMO->L+2 (12%)	H-5->L+1 (3%), H-4->LUMO (3%), H-2->L+2 (6%), H-1->L+1 (4%)
12	236.4	0.0752	H-3->LUMO (28%), H-3->L+2 (24%), H-2->L+1 (10%), H-1->L+2 (10%)	H-5->LUMO (3%), H-4->L+1 (6%)
15	218.2	0.0355	H-5->L+1 (26%), H-4->LUMO (67%)	H-4->L+2 (2%)
18	209.6	0.159	H-5->L+1 (59%), H-4->LUMO (16%)	H-1->L+3 (5%)
19	208.5	0.0546	H-5->LUMO (14%), HOMO->L+3 (66%)	H-4->L+1 (8%), HOMO->L+4 (3%)
20	203.3	0.0568	H-1->L+3 (76%)	H-5->L+1 (2%), H-1->L+4 (5%), HOMO->L+5 (6%)
21	199.4	0.0817	HOMO->L+5 (75%)	H-3->L+3 (5%), H-3->L+4 (2%), H-1->L+3 (5%), HOMO->L+6 (3%)
26	193.1	0.141	H-3->L+3 (14%), H-1->L+4 (32%), HOMO->L+6 (11%), HOMO->L+7 (11%)	H-7->L+1 (3%), H-6->LUMO (3%), H-2->L+5 (8%), H-1->L+3 (3%), H-1->L+8 (3%)
31	184.9	0.0113	H-2->L+4 (26%), H-1->L+5 (16%), H-1->L+7 (12%), HOMO->L+8 (20%)	H-1->L+6 (7%), HOMO->L+4 (3%), HOMO->L+9 (6%)
32	184.8	0.0097	H-2->L+5 (14%), HOMO->L+6 (36%), HOMO->L+7 (35%)	H-1->L+4 (6%)
35	182.4	0.0105	H-2->L+4 (19%), H-1->L+6 (12%), HOMO->L+9 (32%)	H-2->L+3 (3%), H-2->L+8 (3%), H-1->L+5 (5%), H-1->L+7 (5%), HOMO->L+10 (6%)
36	182.0	0.0223	H-9->L+1 (10%), H-7->LUMO (16%), H-6->L+1 (54%)	H-12->L+1 (3%), H-11->L+1 (2%), H-10->LUMO (4%), H-8->LUMO (6%)
37	181.2	0.0101	H-6->L+2 (24%), H-1->L+8 (43%)	H-12->L+2 (3%), H-3->L+3 (2%), H-1->L+4 (7%), HOMO->L+11 (2%), HOMO->L+13 (3%)
40	179.4	0.0411	H-6->L+2 (28%), H-3->L+4 (11%), H-1->L+8 (21%)	H-9->L+2 (2%), H-2->L+5 (5%), H-2->L+6 (5%), H-2->L+7 (4%), HOMO->L+13 (3%)
41	179.2	0.0097	H-3->L+5 (18%), H-1->L+6 (39%), H-1->L+7 (15%)	H-2->L+8 (5%), HOMO->L+9 (4%), HOMO->L+12 (5%)
42	179.0	0.0229	H-9->LUMO (43%), H-7->L+1 (36%)	H-10->L+1 (6%), H-8->L+1 (5%), H-6->L+2 (2%)
46	177.9	0.0254	H-6->L+2 (11%), H-3->L+4 (13%), H-2->L+7 (11%), H-1->L+9 (10%)	H-14->L+2 (2%), H-12->LUMO (2%), H-11->LUMO (4%), H-9->L+2 (4%), H-8->L+1 (9%), H-6->LUMO (3%), H-2->L+5 (7%), H-2->L+6 (9%), H-1->L+8 (4%)
49	175.2	0.0146	H-2->L+8 (55%), HOMO->L+10 (19%)	H-3->L+5 (5%), H-2->L+4 (4%), H-1->L+13 (2%)
50	175.0	0.0311	H-2->L+6 (26%), HOMO->L+11 (15%), HOMO->L+13 (24%)	H-3->L+8 (9%), H-1->L+8 (3%), HOMO->L+14 (5%)
51	174.6	0.0113	H-2->L+8 (12%), HOMO->L+9 (13%), HOMO->L+10 (57%)	H-3->L+5 (3%), H-1->L+7 (4%)
56	173.4	0.0308	H-2->L+6 (11%), H-2->L+7 (56%)	H-2->L+13 (2%), H-1->L+9 (5%), H-1->L+10 (5%), HOMO->L+14 (6%)

N°	$\lambda(\text{nm})$	Oscillator Strength	Major contribution	Minor contribution
59	172.3	0.0124	H-3->L+6 (12%), HOMO->L+12 (58%)	H-2->L+9 (3%), H-1->L+13 (3%), H-1->L+14 (4%)
60	172.0	0.0227	H-9->L+2 (71%), H-6->L+2 (10%)	H-11->L+2 (9%), H-3->L+4 (2%)
65	169.6	0.0387	H-11->L+2 (45%), H-1->L+10 (33%)	H-9->L+2 (4%)
66	169.1	0.0122	H-11->L+2 (27%), H-1->L+10 (29%)	H-9->L+2 (6%), H-1->L+9 (8%), HOMO->L+13 (6%), HOMO->L+14 (9%)
69	168.5	0.0124	H-14->LUMO (28%), H-13->L+1 (38%)	H-12->LUMO (4%), H-8->L+1 (6%), H-7->L+1 (4%), H-3->L+8 (3%), HOMO->L+13 (2%), HOMO->L+14 (5%)
74	167.1	0.0178	H-3->L+8 (29%), H-1->L+12 (13%), HOMO->L+13 (22%), HOMO->L+14 (10%)	H-12->L+2 (3%), H-11->L+2 (2%), H-3->L+4 (2%), H-1->L+10 (5%), HOMO->L+16 (3%)
78	165.3	0.0195	H-12->L+2 (47%)	H-14->L+2 (6%), H-6->L+2 (2%), H-5->L+3 (8%), H-4->L+5 (2%), H-3->L+8 (5%), H-2->L+11 (3%), H-2->L+13 (2%), H-1->L+12 (7%), HOMO->L+14 (5%)
82	163.4	0.0099	H-14->LUMO (17%), H-13->L+1 (15%), H-2->L+11 (43%)	H-12->LUMO (2%), H-2->L+13 (4%), H-1->L+12 (3%), HOMO->L+14 (2%)
89	160.8	0.014	H-4->L+5 (15%), H-3->L+9 (10%), H-3->L+10 (21%), HOMO->L+16 (19%)	H-14->L+2 (3%), H-5->L+3 (3%), H-4->L+6 (4%), H-3->L+12 (4%), H-1->L+12 (7%), HOMO->L+18 (2%)
90	160.7	0.0161	H-5->L+5 (19%), H-4->L+4 (38%), H-2->L+12 (11%)	H-5->L+6 (3%), H-4->L+3 (8%), H-4->L+8 (8%), HOMO->L+17 (3%)
91	160.6	0.0184	H-4->L+5 (37%), H-2->L+13 (13%), HOMO->L+16 (13%)	H-14->L+2 (6%), H-5->L+3 (5%), H-5->L+4 (3%), H-4->L+6 (3%), H-3->L+9 (3%), H-1->L+12 (3%)
95	158.1	0.0741	H-14->L+2 (13%), H-5->L+4 (16%), H-3->L+9 (13%), H-2->L+14 (23%), H-1->L+15 (12%)	H-5->L+3 (3%), H-5->L+8 (3%), H-3->L+10 (6%)
96	157.5	0.0069	H-3->L+11 (14%), H-2->L+12 (10%), H-1->L+14 (10%), HOMO->L+17 (36%)	H-5->L+5 (3%), H-3->L+13 (8%), H-3->L+14 (5%)
97	157.4	0.0109	H-5->L+4 (35%), H-2->L+14 (16%), H-1->L+15 (10%)	H-14->L+2 (8%), H-4->L+5 (7%), H-3->L+9 (2%), H-3->L+12 (2%), HOMO->L+16 (3%)

Table S17. Wavelength (λ , nm) and oscillator strength of the mono-electronic transitions of $[(\text{CH}_3)_2\text{CHOC}(\text{S})\text{S}]_2$ calculated with the TD-B3LYP/6-31+g (d) approximation

N°	$\lambda(\text{nm})$	Oscillator Strength	Major contribution	Minor contribution
5	283.5	0.0231	H-2->LUMO (12%), H-2->L+2 (18%), H-1->L+1 (45%), HOMO->LUMO (18%)	HOMO->L+2 (3%)
9	268.0	0.0569	H-3->L+1 (52%), H-2->LUMO (11%), H-2->L+2 (17%)	HOMO->LUMO (8%), HOMO->L+2 (7%)
11	247.1	0.6605	H-3->L+1 (31%), H-2->LUMO (15%), HOMO->L+2 (16%)	H-5->L+1 (3%), H-4->LUMO (4%), H-2->L+2 (5%), H-1->L+1 (6%)
12	234.6	0.061	H-3->LUMO (21%), H-3->L+2 (25%), H-2->L+1 (11%), H-1->L+2 (10%)	H-5->LUMO (3%), H-4->L+1 (7%), H-1->L+6 (2%), HOMO->L+5 (2%)
13	221.3	0.011	HOMO->L+3 (88%)	H-4->L+1 (4%)
16	217.5	0.0183	H-5->L+1 (29%), H-4->LUMO (39%), H-4->L+2 (27%)	
18	213.4	0.0172	H-5->L+1 (14%), H-1->L+3 (64%)	H-4->LUMO (2%), H-1->L+5 (3%), HOMO->L+4 (7%), HOMO->L+7 (3%)
19	210.9	0.0345	H-5->LUMO (40%), H-4->L+1 (28%)	H-3->LUMO (2%), HOMO->L+3 (6%)
20	208.7	0.1228	H-5->L+1 (37%), H-4->LUMO (19%), H-1->L+3 (21%)	H-3->L+3 (2%)
22	206.0	0.06	HOMO->L+4 (35%), HOMO->L+6 (47%)	H-3->L+3 (2%), H-1->L+3 (5%)
24	200.7	0.0515	H-1->L+5 (55%), HOMO->L+4 (10%)	H-3->L+3 (4%), H-2->L+4 (2%), H-2->L+6 (4%), H-1->L+3 (2%), H-1->L+8 (4%), HOMO->L+6 (6%)
25	199.6	0.0094	H-1->L+5 (14%), HOMO->L+4 (35%), HOMO->L+6 (36%)	H-2->L+6 (4%), H-1->L+3 (3%)
26	198.5	0.0091	H-2->L+3 (16%), H-2->L+5 (18%), H-1->L+4 (12%), H-1->L+6 (36%)	H-6->LUMO (3%), H-2->L+8 (3%), H-2->L+9 (2%)
27	196.3	0.0157	H-3->L+3 (63%), HOMO->L+7 (14%)	H-1->L+5 (3%), HOMO->L+4 (9%)
29	193.9	0.0097	H-2->L+5 (13%), H-1->L+4 (54%), HOMO->L+8 (21%)	HOMO->L+10 (3%)
32	192.2	0.0242	H-3->L+3 (15%), HOMO->L+7 (73%)	
33	190.5	0.0131	H-2->L+4 (15%), H-2->L+6 (36%), H-1->L+5 (13%)	H-7->LUMO (3%), H-6->L+1 (3%), H-3->L+3 (4%), H-3->L+5 (5%), H-1->L+8 (5%), H-1->L+9 (3%)
35	187.9	0.0151	H-1->L+7 (41%), HOMO->L+10 (35%)	H-3->L+4 (4%), H-1->L+4 (8%)
37	186.7	0.0289	H-3->L+5 (22%), H-2->L+4 (46%), H-1->L+8 (13%)	H-1->L+10 (3%), HOMO->L+11 (5%)
38	184.7	0.0499	H-3->L+5 (24%), H-1->L+8 (41%), H-1->L+9 (14%)	HOMO->L+6 (3%), HOMO->L+12 (5%)
42	183.2	0.0159	H-2->L+4 (11%), H-1->L+10 (10%), HOMO->L+11 (33%), HOMO->L+12 (20%)	H-2->L+6 (7%), H-1->L+8 (6%)
48	178.8	0.0201	H-8->L+1 (10%), H-7->L+1 (37%), H-6->LUMO (24%), H-6->L+2 (12%)	H-3->L+4 (4%), H-3->L+6 (4%)
49	178.6	0.0328	H-2->L+7 (29%), H-1->L+9 (22%), HOMO->L+12 (28%)	H-2->L+4 (3%), HOMO->L+11 (7%)
50	177.7	0.0139	H-6->L+2 (66%), H-2->L+8 (10%)	H-3->L+4 (4%), H-3->L+6 (7%), H-2->L+9 (3%)
51	176.77	0.0506	H-1->L+10 (29%), HOMO->L+12 (12%), HOMO->L+14 (25%)	H-3->L+8 (6%), H-3->L+9 (4%), H-2->L+7 (2%),

continuation of the Table S17

N°	$\lambda(\text{nm})$	Oscillator Strength	Major contribution	Minor contribution
				H-2->L+12 (3%), HOMO->L+11 (3%)
53	176.27	0.0149	H-1->L+11 (42%), HOMO->L+13 (14%)	H-3->L+4 (8%), H-2->L+9 (2%), H-2->L+10 (6%), H-1->L+12 (8%), HOMO->L+10 (8%)
55	174.0	0.0165	H-3->L+7 (39%), H-1->L+11 (25%)	H-4->L+3 (3%), H-3->L+4 (2%), H-2->L+10 (7%), H-1->L+12 (9%), HOMO->L+13 (3%), HOMO->L+15 (2%)
60	172.8	0.0145	H-3->L+8 (41%), HOMO->L+14 (21%)	H-7->L+2 (2%), H-3->L+5 (3%), H-3->L+9 (3%), H-1->L+9 (3%), H-1->L+10 (3%), H-1->L+13 (2%), HOMO->L+12 (4%), HOMO->L+18 (5%)
61	172.5	0.0106	H-8->L+1 (17%), HOMO->L+15 (38%)	H-6->LUMO (3%), H-3->L+7 (4%), H-2->L+9 (4%), H-2->L+10 (2%), H-1->L+12 (3%), H-1->L+14 (4%), HOMO->L+13 (8%), HOMO->L+17 (4%)
70	167.0	0.0338	H-3->L+10 (17%), H-2->L+12 (25%), H-1->L+13 (17%), H-1->L+15 (23%)	H-3->L+9 (2%), HOMO->L+18 (3%)
71	166.9	0.0128	H-2->L+11 (11%), H-2->L+12 (28%), H-1->L+15 (10%), HOMO->L+16 (23%)	H-3->L+8 (2%), H-2->L+14 (3%), H-1->L+13 (4%), HOMO->L+14 (4%), HOMO->L+18 (4%)
73	166.6	0.021	H-3->L+9 (34%), HOMO->L+16 (20%), HOMO->L+18 (19%)	H-3->L+8 (5%), H-1->L+13 (7%), HOMO->L+14 (3%)
77	164.5	0.0181	H-8->L+2 (11%), H-5->L+5 (10%), H-3->L+10 (24%), H-1->L+15 (20%)	H-5->L+3 (3%), H-2->L+12 (5%), HOMO->L+18 (9%)
83	163.1	0.0643	H-8->L+2 (32%), H-5->L+5 (11%), H-4->L+6 (11%), H-3->L+10 (15%)	H-4->L+4 (4%), H-2->L+12 (3%), H-2->L+14 (2%)
87	161.7	0.035	H-11->LUMO (24%), H-9->L+1 (39%)	H-12->LUMO (4%), H-5->L+5 (4%), H-4->L+4 (3%), H-2->L+14 (4%), H-1->L+17 (6%)
94	159.4	0.0199	H-11->L+2 (12%), H-8->L+2 (20%), H-5->L+5 (12%), H-4->L+4 (30%)	H-12->L+2 (3%), H-11->LUMO (3%), H-9->L+1 (2%), H-4->L+6 (3%), H-2->L+14 (4%), H-2->L+16 (3%)

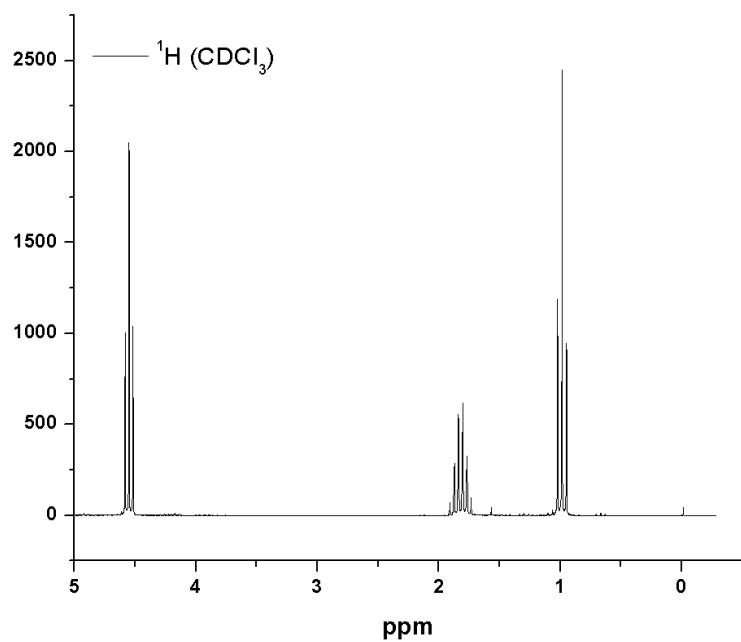


Figure S1. ^1H NMR spectra of $[\text{CH}_3(\text{CH}_2)_2\text{OC}(\text{S})\text{S}]_2$ in CDCl_3 .

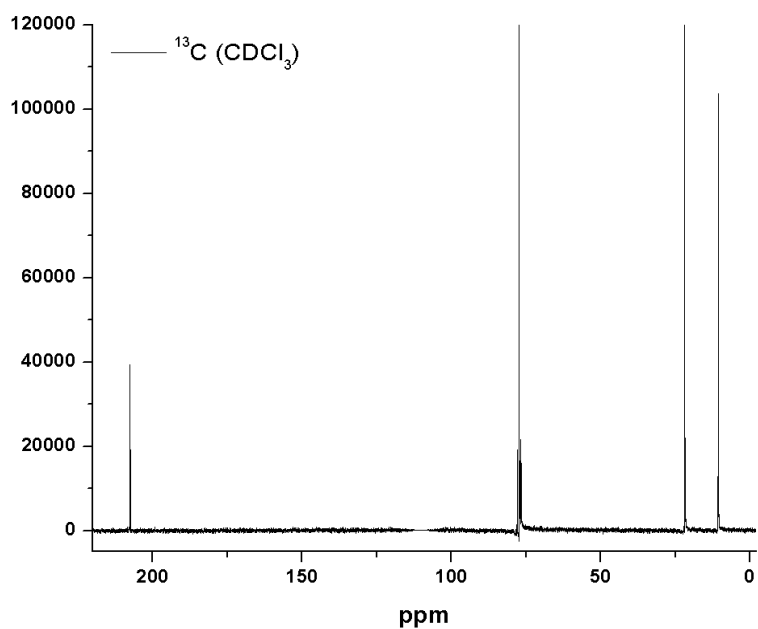


Figure S2. ^{13}C NMR spectra of $[\text{CH}_3(\text{CH}_2)_2\text{OC}(\text{S})\text{S}]_2$ in CDCl_3 .

(b)

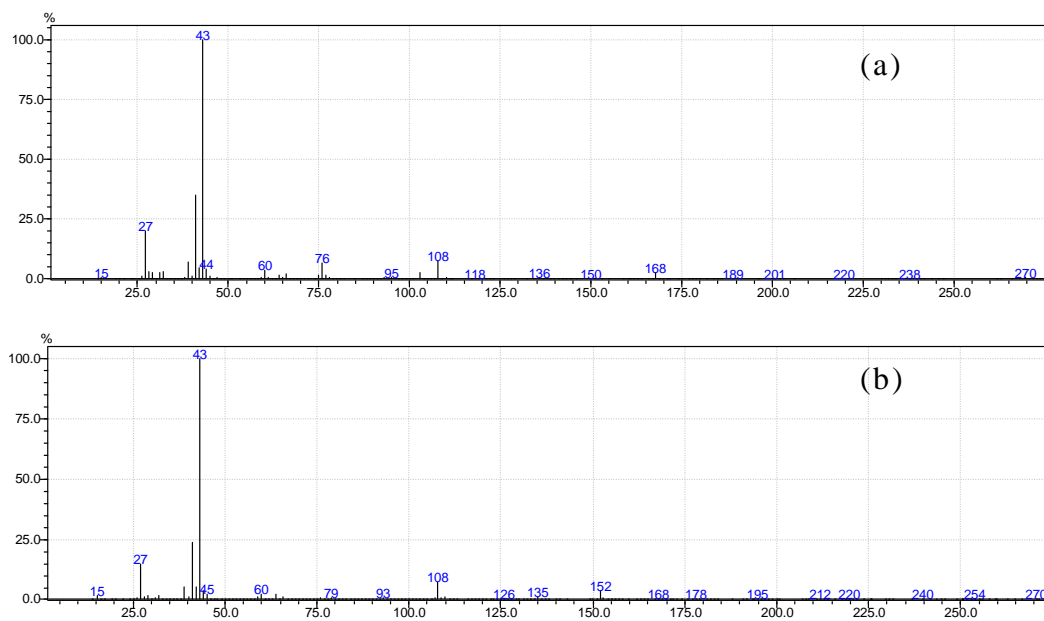
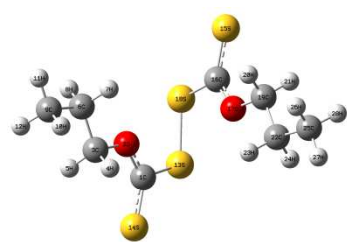
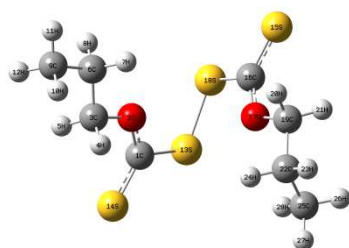


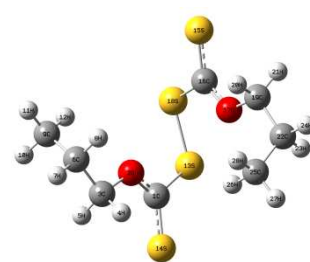
Figure S3. Mass spectra of $[\text{CH}_3(\text{CH}_2)_2\text{OC}(\text{S})\text{S}]_2$ (a) and $[(\text{CH}_3)_2\text{CHOC}(\text{S})\text{S}]_2$ (b), on electron impact ionization (70 eV, ion source temperature = 200 °C).



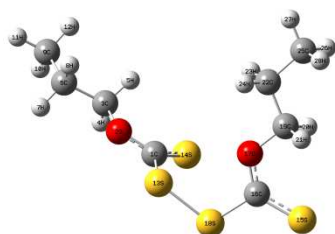
I (AAAGAAA)



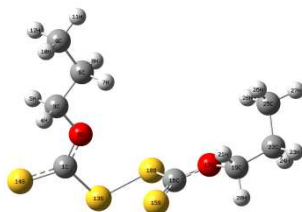
II (AAAGAAG⁺)



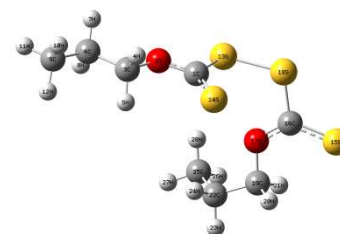
III (G⁺AAGAAG⁻)



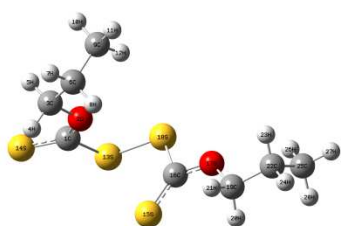
IV (AASGAAA)



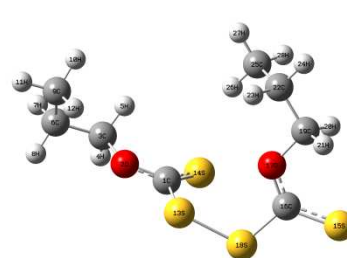
V (AASGAAG⁺)



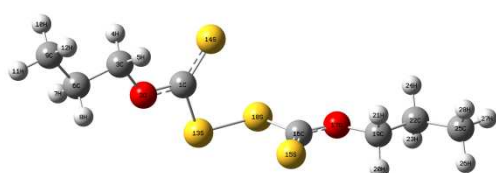
VI (AAAGSAG⁺)



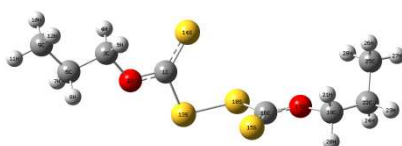
VII (G⁺AAGSAG⁻)



VIII (G⁺ASGAAG⁻)



IX (AASGSAA)



X (AASGSAG⁺)



XI (G⁺ASGSAG⁻)

Figure S4. Molecular models of the most stable conformers of $[\text{CH}_3(\text{CH}_2)_2\text{OC}(\text{S})\text{S}]_2$ calculated with the B3LYP/6-31+G* approximation.

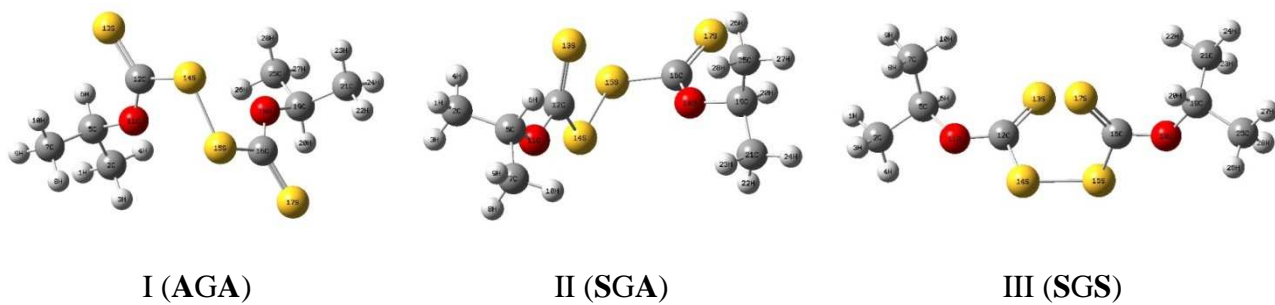


Figure S5. Molecular models of the most stable conformers of $[(\text{CH}_3)_2\text{CHOC}(\text{S})\text{S}]_2$ calculated with the B3LYP/6-31+G* approximation.

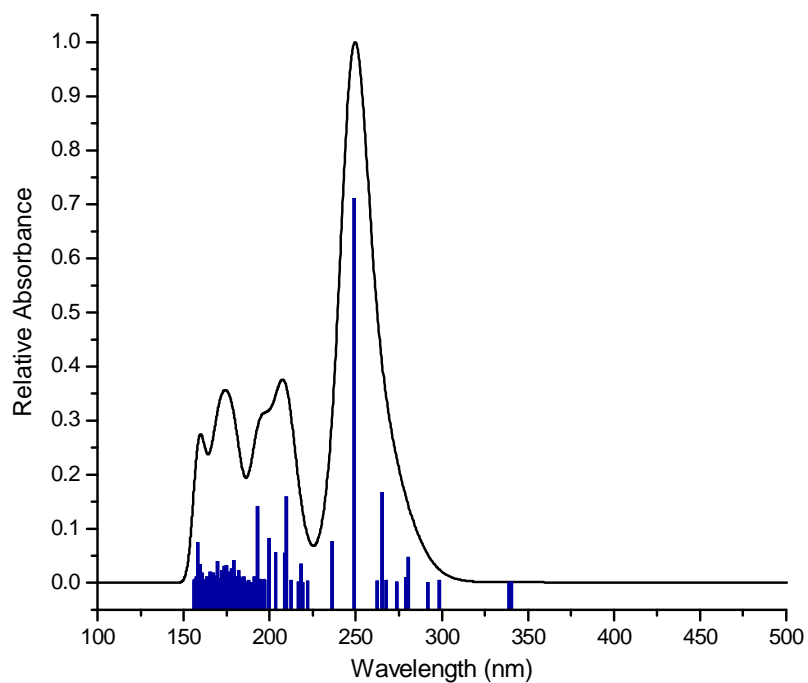


Figure S6. Absorption spectra (full trace) and oscillator strength of the electronic transitions (blue bars) of $[\text{CH}_3(\text{CH}_2)_2\text{OC}(\text{S})\text{S}]_2$ calculated with the TD-B3LYP/6-31+G* approximation.

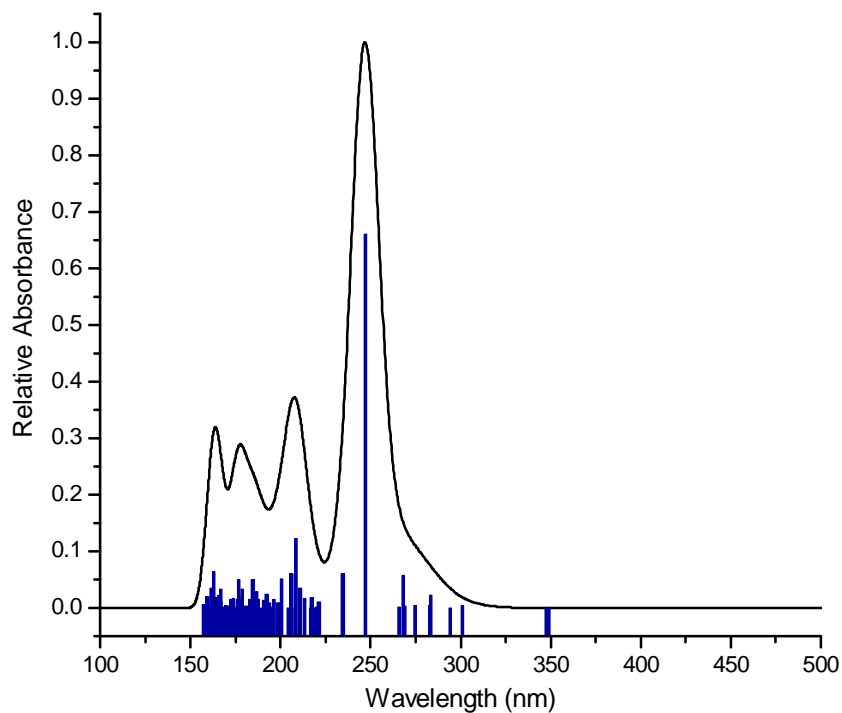


Figure S7. Absorption spectra (full trace) and oscillator strength of the electronic transitions (blue bars) of $[(\text{CH}_3)_2\text{CHOC}(\text{S})\text{S}]_2$ calculated with the TD-B3LYP/6-31+G* approximation.